

TOPOLOGICAL DESIGN OF AN ASYMMETRIC 3-TRANSLATIONAL PARALLEL MECHANISM WITH ZERO COUPLING DEGREE AND MOTION DECOUPLING

Huiping Shen

School of Mechanical Engineering, Changzhou
University, Changzhou 213016, China
shp65@126.com

Chengqi Wu

School of Mechanical Engineering, Changzhou
University, Changzhou 213016, China
753272704@qq.com

Damien Chablat

CNRS, Laboratoire des
Sciences du Numérique de
Nantes, UMR 6004
Nantes, France
Damien.Chablat@cnrs.fr

Guang Lei Wu

School of Mechanical
Engineering, Dalian University of
Science and Technology, Dalian
116031, China
gwu@dlut.edu.cn

Ting-li Yang

School of Mechanical
Engineering, Changzhou
University, Changzhou 213016,
China
yangtl@126.com

ABSTRACT

In this paper a new asymmetric 3-translational (3T) parallel manipulator, i.e., RPa(3R) 2R+RPa, with zero coupling degree and decoupled motion is firstly proposed according to topology design theory of parallel mechanism (PM) based on position and orientation characteristics (POC) equations. The main topological characteristics such as POC, degree of freedom and coupling degree are calculated. Then, the analytical formula for the direct and inverse kinematic are directly derived since coupling degree of the PM is zero. The study of singular configurations is simple because of the independence of the kinematic chains.

INTRODUCTION

In many industrial production lines, process operations require pure translation movements only. Therefore, the 3-DOF translational parallel mechanism (TPM) has a significant potential value since it is a relatively simple structure and easily controlled [1].

Many scholars have been studying the TPM. For example: original design of 3-DOF TPM is the Delta Robot which was presented by Clavel [2]. The structure manipulators of TPM have been developed [3-5]. Tsai et al [6] presented the 3-DOF TPM, the moving actuators are prismatic joints and the sub-chain is 4R parallelogram mechanism (P is prismatic joint and R is revolute joint). The same architecture was optimized to have isotropic posture in the center of its workspace with 3 or 5 degrees of freedom in [7, 8]. Li et al developed a 3-UPU parallel mechanism (U is universal joint) [9] and analyzed the instantaneous kinematics performance of the TPM. In [10], the authors suggested a 3-RRC TPM and developed the forward and inverse solution equation (C is cylindrical joint). Considering the anisotropy of kinematics, Zhao et al [11] analyzed the dimension synthesis and kinematics of the 3-DOF TPM based on the Delta PM. Zeng et al [12-14] introduced a 3-DOF TPM called as Tri-pyramid robot and presented a more detailed analytical approach for the Jacobi matrix. G. Bhutani et al [15] established a new design for the 3-UPU mechanism by taking into account mathematical models. Gao et al [16] developed a TPM with decoupled motion.

However, the most previous TPMs generally suffer from two major problems: i) the degree of coupling κ of the mechanism is greater than zero, which means its forward position solution is generally not analytical, and ii) the mechanism does not have input-output decoupling characteristics [17], which leads to the complexity of motion control and path planning.

According to topology design theory of PM based on position and orientation characteristics (POC) equations [18], a new TPM is proposed in this paper. The TPM is designed with simple structure and features zero coupling degree, which makes it possible to produce analytical models for the direct and inverse kinematic model. In addition, TPM's motion control and trajectory planning is easier thanks to its partially decoupled motion characteristics.

STRUCTURAL DESIGN

The 3T parallel manipulator proposed in this paper is illustrated in Fig.1. The base platform 0 is connected to the moving platform 1 by two hybrid simple opened chain (HSOCs).

To illustrate the structure of the manipulator, the CAD design of the hybrid chain is shown in Fig. 1(A). Two HSOCs composed of series of links are shown in Fig. 1(B).

The first HSOC includes the branches I and II: The shorter link 3 of a parallelogram composed of four spherical pairs (S_a , S_b , S_c and S_d) is connected at point a, by actuated arm 2, to the base 0 by a revolute joint R_{11} . The extended part of the opposite link 3' of the parallelogram is connected in parallel with a sub-chain composed of two links(6 and 5) and three parallel revolute joints (3R, i.e., $R_{23}PR_{22}PR_{21}$), which is denoted as $RP_a^{(4S)}3R$. Further, two links (7 and 8) and two parallel revolute joints (2R, i.e., $R_{12} \parallel R_{13}$) are connected in series with the link 3', which are connected to the moving platform 1. Because the two revolute joints(2R, i.e., $R_{11} \perp R_{21}$) of the base 0 are perpendicular to each other the HSOC can be recorded as $RP_a^{(4S)}3R \perp 2R$, the end part of which is part of the moving platform 1 and produce three translations and one rotation.

The second HSOC includes the branch III: The parallelogram composed of four revolute joints (R_e , R_f , R_g and R_h) is connected in series with two parallel revolute joints (2R, i.e., $R_{32} \parallel R_{31}$), and is connected to the moving platform 1 by R_{33} ($R_{33} \parallel R_{32}$). The HSOC can be recorded as $RP_a^{(4R)}$, the end part of which produce three translations and one rotation. It is obvious that the HSOC has the same branch as the typical Delta (but the Delta contains three such complex HSOCs).

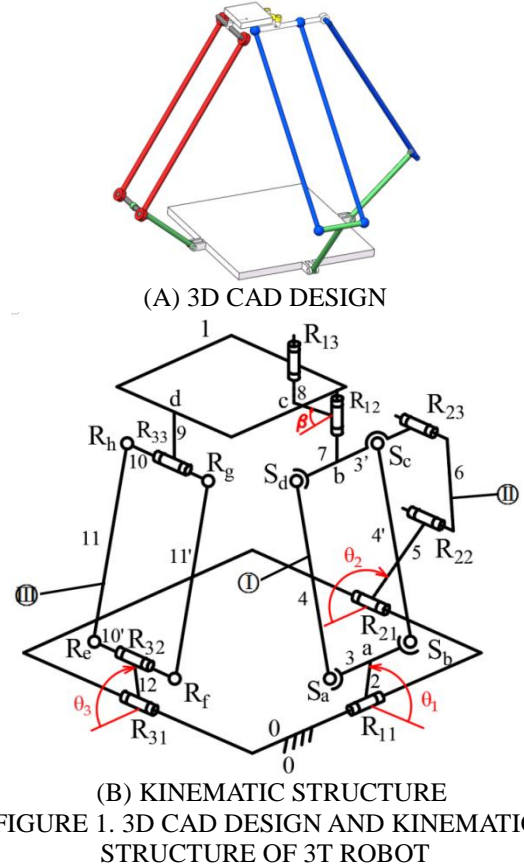


FIGURE 1. 3D CAD DESIGN AND KINEMATIC STRUCTURE OF 3T ROBOT

TOPOLOGICAL ANALYSIS

Analysis of the POC set

The POC set equations for serial and parallel mechanisms are expressed respectively as follows:

$$M_{bi} = \prod_{i=1}^m M_{Ji} \quad (1)$$

$$M_{Pa} = \prod_{i=1}^n M_{bi} \quad (2)$$

where

M_{Ji} - POC set generated by the i -th joint;

M_{bi} - POC set generated by the end link of i -th branched chain;
 M_{pa} - POC set generated by the moving platform of PM.

The topological architecture of the two *HSOCs* of the mechanism can be denoted as:

- ① $HSOC_1\{R_{11}(-P^{4S}-P^{4S}-R^{4S}-R^{4S})-(R_{23}\parallel R_{22}\parallel R_{21})\perp(R_{12}\parallel R_{13})\}$
 ② $HSOC_2\{R_{31}(P^{(4R)})PR_{32}PR_{33}\}$.

The POC sets of the end of the two *HSOCs* are determined according to Eqs.(1) and (2) as follows:

$$M_{HSOC_1} = \left[\begin{array}{c} t^1(\perp R_{11}) \\ r^1(PR_{11}) \end{array} \right] \cup \left[\begin{array}{c} t^1(P\langle abcd \rangle) \cup t^1(\perp(ab)) \\ r^1(P(ab)) \cup r^1(\perp(bd)) \end{array} \right]$$

$$\cap \left[\begin{array}{c} t^2(\perp R_{23}) \\ r^1(PR_{21}) \end{array} \right] \cup \left[\begin{array}{c} t^2(\perp R_{12}) \\ r^1(PR_{12}) \end{array} \right] = \left[\begin{array}{c} t^3 \\ r^1(PR_{12}) \end{array} \right]$$

$$M_{HSOC_2} = \left[\begin{array}{c} t^1(\perp R_{31}) \\ r^1(PR_{31}) \end{array} \right] \cup \left[\begin{array}{c} t^1(\perp R_{32}) \\ r^1(PR_{32}) \end{array} \right] \cup \left[\begin{array}{c} t^1(\perp R_{33}) \\ r^1(PR_{33}) \end{array} \right] \cup \left[\begin{array}{c} t^1(PR_{32}) \\ r^0 \end{array} \right]$$

$$= \left[\begin{array}{c} t^3 \\ r^1(PR_{31}) \end{array} \right]$$

The POC set of the moving platform of this PM is determined from Eq.(2) by

$$M = M_{HSOC_1} \cap M_{HSOC_2} = \left[\begin{array}{c} t^3 \\ r^0 \end{array} \right]$$

So, the moving platform 1 of the PM produces a pure translation motion.

Determining the DOF

The general and full-cycle DOF formula for PMs proposed in author's work[18] is given:

$$F = \sum_{i=1}^m f_i - \sum_{j=1}^v \xi_{L_j} \quad (3a)$$

$$\sum_{j=1}^v \xi_{L_j} = \dim \left\{ \left(\prod_{i=1}^j M_{b_i} \right) \cup M_{b(j+1)} \right\} \quad (3b)$$

where, F - DOF of PM. f_i - DOF of the i th joint. m - number of all joints of the PM. v - number of independent loops ($v=m-n+1$, n - number of links). ξ_{L_j} - number of independent equations of the j th loop. $\prod_{i=1}^j M_{b_i}$ - POC set generated by the sub-PM formed by the former j branches; $M_{b(j+1)}$ - POC set generated by the end link of $j+1$ sub-chains.

The mechanism can be broken down into two independent loops, and their constraint equations are calculated as follows:

① The first independent loop is consisted of branch I and II, the *HSOC*₁ is deduced as:

$$HSOC_1\{R_{11}(P^{4S}-P^{4S}-R^{4S}-R^{4S}-R_{23}\parallel R_{22}\parallel R_{21})\}$$

Thus, as obtained from Eq. (2), the POC set of the sub PM is

$$M_{pa(1-2)} = M_I \cap M_{II} = \dim \left\{ \left[\begin{array}{c} t^2 \\ r^2 \end{array} \right] \cap \left[\begin{array}{c} t^2(\perp R_{21}) \\ r^1(PR_{21}) \end{array} \right] \right\} = \left[\begin{array}{c} t^2 \\ r^0 \end{array} \right] \quad (4)$$

In accordance with Eq. (3), the independent constraint equation numbers ξ_{L_1} and the DOF, respectively, can be obtained as follows:

$$\begin{aligned} \zeta_{L_1} &= \dim \{M_I \cup M_{II}\} \\ &= \dim \left\{ \left[\begin{array}{c} t^2 \\ r^2 \end{array} \right] \cup \left[\begin{array}{c} t^2(\perp R_{21}) \\ r^1(PR_{21}) \end{array} \right] \right\} \\ &= \dim \left\{ \left[\begin{array}{c} t^3 \\ r^3 \end{array} \right] \right\} = 6 \end{aligned}$$

$$F = \sum_{i=1}^m f_i - \sum_{j=1}^1 \zeta_{L_j} = 8 - 6 = 2.$$

It can be seen that the output link 3' of the sub PM produces two dimensional translational motions in the xoz plane, and is only determined by the active joints R_{11} and R_{21} . Therefore, the mechanism has partial motion decoupling.

② The above-mentioned sub PM and the branch chain III comprise the second loop:

$$HSOC_2\{R_{31}(P^{(4R)})\parallel R_{32}\parallel R_{33} - R_{13}\parallel R_{12}\}$$

In accordance with Eq. (3), the independent displacement equation numbers ξ_{L_2} and the DOF, respectively, can be obtained as follows:

$$\begin{aligned} \xi_{L_2} &= \dim \left\{ \left[\begin{array}{c} t^2(\perp R_{12}) \\ r^1(PR_{13}) \end{array} \right] \cup M_{III} \right\} = \dim \left\{ \left[\begin{array}{c} t^2(\perp R_{12}) \\ r^1(PR_{13}) \end{array} \right] \cup \left[\begin{array}{c} t^3 \\ r^1(PR_{31}) \end{array} \right] \right\} \\ &= \dim \left\{ \left[\begin{array}{c} t^3 \\ r^2(P\langle R_{13}, R_{31} \rangle) \end{array} \right] \right\} = 5 \end{aligned}$$

$$F = \sum_{i=1}^m f_i - \sum_{j=1}^2 \zeta_{L_j} = (8+6) - (6+5) = 3.$$

Determining the coupling degree

Definition of coupling degree

According to the composition principle of mechanism based on SOC units, any PM can be decomposed into a series of Assur kinematics chains (AKCs), and an AKC with ν independent loops can be broken down into ν single-open-chains (SOC). The constraint of the j^{th} SOC is defined by

$$\Delta_j = \sum_{i=1}^{m_j} f_i - I_j - \zeta_{L_j} = \begin{cases} \Delta_j^- = -5, -4, -2, -1 \\ \Delta_j^0 = 0 \\ \Delta_j^+ = +1, +2, +3, \dots \end{cases} \quad (4)$$

where, m_j - number of joints contained in the j^{th} SOC; f_i - DOF of the i^{th} joints; I_j - number of actuated joints in the j^{th} SOC; ζ_{L_j} - number of independent equations of the j^{th} loop.

Then, the coupling degree of AKC is

$$\kappa = \frac{1}{2} \min \left\{ \sum_{j=1}^{\nu} |\Delta_j| \right\} \quad (5)$$

The physical meaning of the coupling degree κ can be explained as follows:

① The coupling degree κ reflects the correlation and dependence between kinematic variables of each independent loop of the mechanism. It has been proved that the higher κ , the greater the complexity of the kinematic and dynamic problems of the mechanism will be.

② For $\kappa=0$, the motion of each loop can be obtained independently, and we can finally obtain the solution of the direct kinematic model; If $\kappa>0$, this means that the direct kinematic model must be solved using several constraint equations.

Calculation of coupling degree

The independent displacement equations $\xi_{L_i} (i=1, 2)$ of loop 1 and loop 2 have been calculated in the previous section, i.e., $\xi_{L_1}=6$, $\xi_{L_2}=5$, thus, the both coupling degrees are calculated by Eq. (4), respectively

$$\Delta_1 = \sum f_i - I_j - \zeta_{L_j} = (5+3) - 2 - 6 = 0$$

$$\Delta_2 = \sum f_i - I_j - \zeta_{L_j} = 6 - 1 - 5 = 0$$

By Eq.(5), it can be seen that the mechanism contains two AKCs with zero coupling degree ($\kappa_1=0$, $\kappa_2=0$), hence, the closed-form forward position solution of the PM can be easily obtained by AKC₁ and AKC₂.

POSITION ANALYSIS

Establishment of the coordinate system and parameterization

To simplify reading, the mechanism shown in Fig. 1 is developed under a planar view in the Fig. 2. The base 0 and the moving platform 1 are square shaped, and the sizes of their sides are $2l_1$ and $2l_2$, respectively. The three revolute joints (3R, i.e., R_{11} , R_{21} and R_{31}) of the base 0 are distributed at the midpoint of each edge.

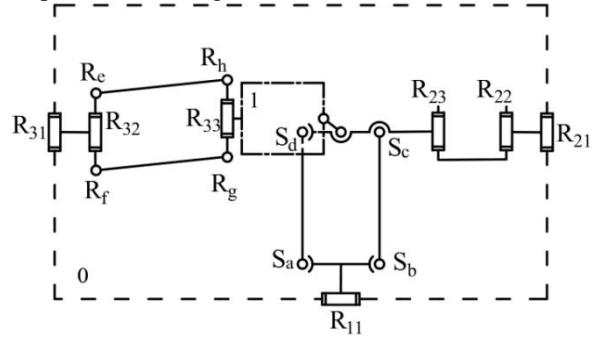


FIGURE 2. A PLANAR VIEW OF THE 3 ROBOTS

Without losing the generality, the frame coordinate system $O-xyz$ is established on the base 0. The x -axis is parallel to the axis of R_{11} , and the y -axis is perpendicular to the axis of R_{11} .

On the moving platform 1, the moving coordinate system uvw is established at P . The u axis and the v axis are perpendicular and parallel to the axis of the R_{33} respectively. Both z and w axis are determined by the right hand Cartesian coordinate rule, as shown in Fig. 3(A). For ease of comprehension, the 3T PM is redesigned in 3D view as shown in Fig. 3(B).

The length of each actuated arms 2, 5 and 12 is

$$A_1B_1 = A_2B_2 = A_3B_3 = l_3 \text{ with } l_3 \neq l_1$$

The length of driven links 6 and the length of longer links of the both parallelograms 4 and 11 are

$$B_1C_1 = B_2C_2 = B_3C_3 = l_4$$

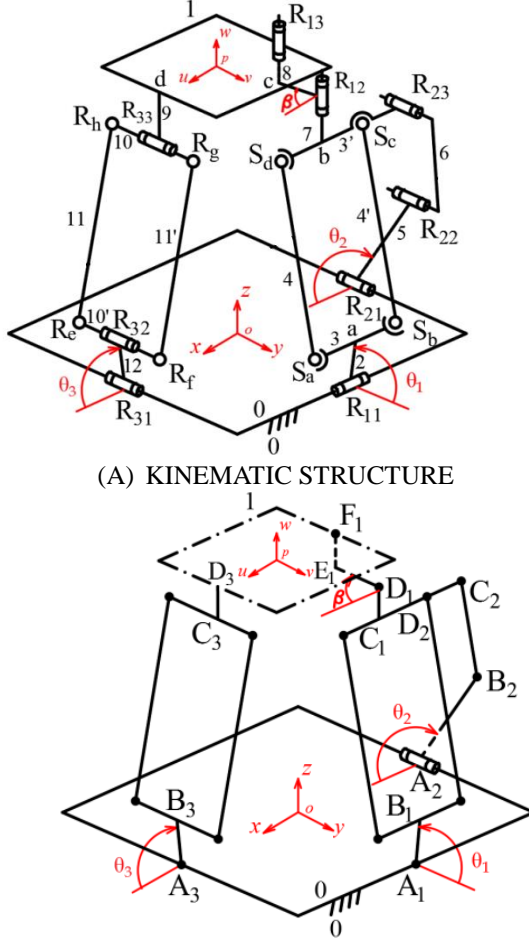
The shorter links of the parallelogram are $2l_5$ and the point B_i and $C_i (i=1, 2, 3)$ are the midpoint of the short edge. Thus, the parameters of the other links are respectively defined below. $C_2D_2 = l_5$, $C_1D_1 = C_3D_3 = E_1F_1 = l_6$, $D_1E_1 = l_7$.

The three input angles are defined as θ_1 , θ_2 and θ_3 , as shown in Fig. 3(a). That is, the angle between the vectors A_1B_1 and the

y-axis is θ_1 . The angles between the vectors A_2B_2 , A_3B_3 , and the x-axis are θ_2 and θ_3 respectively. The angle between the vectors D_1E_1 and the x-axis is β .

Direct kinematics

To solve the direct kinematic problem, i.e., to compute the position of the moving platform, we set the values of the actuated joints θ_1 , θ_2 and θ_3 .



(A) KINEMATIC STRUCTURE

(B) KINEMATIC MODELING

FIGURE 3. PARAMETERIZATIONS OF THE 3T PM

Direct kinematics of AKC_1

The coordinates of A_1 , A_2 and A_3 on the base platform 1 are

$$A_1 = [0 \ l_1 \ 0]^T, \quad A_2 = [-l_1 \ 0 \ 0]^T \quad \text{and} \quad A_3 = [l_1 \ 0 \ 0]^T.$$

The coordinates of each end-point of the three actuated arms 2, 5 and 12, i.e., B_1 , B_2 and B_3 are easily calculated as

$$B_1 = [0 \ l_1 + l_3 \cos \theta_1 \ l_3 \sin \theta_1]^T,$$

$$B_2 = [-l_1 + l_3 \cos \theta_2 \ 0 \ l_3 \sin \theta_2]^T,$$

$$B_3 = [l_1 + l_3 \cos \theta_3 \ 0 \ l_3 \sin \theta_3]^T$$

As stated in Eq. (4), the output link 3' of the sub-PM can only produce two dimensional translational motions in the xoz plane, i.e. $y_{C_1} = y_{C_2} = 0$. Due to the link length constraints defined by $B_1C_1 = B_2C_2 = l_4$, there are two constraint equations as below.

$$\begin{cases} (x_{C_1} - x_{B_1})^2 + (y_{C_1} - y_{B_1})^2 + (z_{C_1} - z_{B_1})^2 = l_4^2 \\ (x_{C_2} - x_{B_2})^2 + (y_{C_2} - y_{B_2})^2 + (z_{C_2} - z_{B_2})^2 = l_4^2 \end{cases} \quad (6)$$

Equation (6) leads to:

$$a_1 x_{C_1} + b_1 z_{C_1} = c_1 \quad (7)$$

Where

$$a_1 = 2(x_{B_2} + 2l_5), \quad b_1 = 2(z_{B_2} - z_{B_1}),$$

$$c_1 = (x_{B_2} + 2l_5)^2 + z_{B_2}^2 - y_{B_1}^2 - z_{B_1}^2$$

If $a_1=0$ and $b_1=0$, then $c_1 = -y_{B_1}^2 = 0$. But y_{B_1} could not be zero. Hence, a_1 and b_1 are not zero at the same time, and we can have two cases as follows:

① $a_1 = 0$. In such a case, we have

$$\begin{cases} z_{C_1} = c_1 / b_1 \\ x_{C_1} = \pm \sqrt{l_4^2 - (z_{B_1} - z_{C_1})^2 - y_{B_1}^2} \end{cases} \quad (8a)$$

② $a_1 \neq 0$. In such a case, we have

$$\begin{cases} z_{C_1} = \frac{e_1 \pm \sqrt{e_1^2 - 4d_1 f_1}}{2d_1} \\ z_{C_1} = \frac{c_1 - b_1 z_{C_1}}{a_1} \end{cases} \quad (8b)$$

where

$$d_1 = a_1^2 + b_1^2, \quad e_1 = 2(b_1 c_1 + z_{B_1} a_1^2), \quad f_1 = a_1^2 (y_{B_1}^2 + z_{B_1}^2 - l_4^2) + c_1^2.$$

Direct kinematics of AKC_2

From the Fig. 3, the coordinates of D_1 , E_1 , F_1 , D_3 , and C_3 are defined as:

$$D_1 = [x_{C_1} \ 0 \ z_{C_1} + l_6]^T,$$

$$E_1 = [x_{D_1} + l_7 \cos \beta \ l_7 \sin \beta \ z_{D_1}]^T,$$

$$F_1 = [x_{D_1} + l_7 \cos \beta \ l_7 \sin \beta \ z_{D_1}]^T,$$

$$D_3 = [x_{D_1} + l_7 \cos \beta + 2l_2 \ l_7 \sin \beta \ z_{D_1}]^T,$$

$$C_3 = [x_{D_3} \ y_{D_3} \ y_{D_3} - l_6]^T.$$

Due to the link length constraints defined by $B_3C_3=l_4$, the constraint equation can be deduced as below.

$$(x_{B_3}-x_{C_3})^2+(y_{B_3}-y_{C_3})^2+(z_{B_3}-z_{C_3})^2=l_4^2 \quad (9)$$

Equation (9) leads to

$$a_2 \cos \beta = b_2 \quad (10)$$

With

$$a_2 = 2l_7(x_{D_1}-x_{B_3}+2l_2) \quad ,$$

$$b_2 = l_4^2 - l_7^2 - (x_{D_1}-x_{B_3}+2l_2)^2 - (z_{D_1}-z_{B_3})^2$$

After β is obtained by Eq. (10), the coordinate of D_3 and F_1 can be obtain. Thus, the coordinates of P on the platform is

$$\begin{cases} x = (x_{D_3} + x_{F_1}) / 2 \\ y = (y_{D_3} + y_{F_1}) / 2 \\ z = (z_{D_3} + z_{F_1}) / 2 \end{cases} \quad (11)$$

Inverse kinematics

To solve the inverse kinematics, we compute the values of θ_1 , θ_2 and θ_3 as a function of the coordinate P of the moving platform. We have also to evaluate the value of β , which is a passive variable form the Eq. (10).

Solution for β

For a given position of the moving platform, there are two positions for points C_1 and C_2 with

$$\beta = \arcsin\left(\frac{y_{D_3}}{l_7}\right) \quad \text{or} \quad \beta = \pi - \arcsin\left(\frac{y_{D_3}}{l_7}\right)$$

For each position of C_1 and C_2 , we can calculate θ_1 and θ_2 .

Solution for θ_1 and θ_2 :

From Fig. 3, the coordinates of F_1 , E_1 and D_1 are

$$F_1 = [x-l_2, y, z]^T, \quad E_1 = [x-l_2, y, z-l_6]^T, \quad D_1 = [x_{D_1}, 0, z-l_6]^T.$$

Due to the link length constraints defined by $D_1E_1=l_7$, the coordinates of D_1 , C_1 and C_2 can be deduced as below:

$$D_1 = \left[x-l_2 + \sqrt{l_7^2 - y^2} \quad 0 \quad z-l_6 \right]^T$$

$$C_1 = [x_{D_1} \quad 0 \quad z_{D_1}-l_6]^T, \quad C_2 = [x_{D_1}-2l_5 \quad 0 \quad z_{D_1}-l_6]^T.$$

Then, due to the link length constraints defined by $B_1C_1=B_2C_2=l_4$, i.e.

$$\begin{cases} (x_{C_1}-x_{B_1})^2+(y_{C_1}-y_{B_1})^2+(z_{C_1}-z_{B_1})^2=l_4^2 \\ (x_{C_2}-x_{B_2})^2+(y_{C_2}-y_{B_2})^2+(z_{C_2}-z_{B_2})^2=l_4^2 \end{cases} \quad (12)$$

Then, Eq. (12) leads to:

$$\theta_i = 2 \arctan\left(\frac{2l_3z_i \pm \sqrt{4z_i^2l_3^2 - g_i h_i}}{g_i}\right), \quad \text{for } i=1, 2 \quad (13)$$

where

$$z_1 = z_{C_1}, \quad z_2 = z_{C_2}, \quad h_1 = (l_1-l_3)^2 - l_4^2 + x_{C_1}^2 + z_{C_1}^2,$$

$$g_1 = (l_1+l_3)^2 - l_4^2 + x_{C_1}^2 + z_{C_1}^2, \quad ,$$

$$h_2 = (l_1-l_3)^2 - l_4^2 + x_{C_2}^2 + z_{C_2}^2 + 2x_{C_2}(l_1-l_3),$$

$$g_2 = (l_1+l_3)^2 - l_4^2 + x_{C_2}^2 + z_{C_2}^2 + 2x_{C_2}(l_1+l_3).$$

Solution for θ_3

Similarly, the coordinates of D_3 and C_3 can be easily obtained

$$D_3 = [x+l_2, y, z]^T, \quad C_3 = [x+l_2, y, z-l_6]^T.$$

Due to the link length constraints defined by $B_3C_3=l_4$, the constraint equation is established as below.

$$(x_{C_3}-x_{B_3})^2+(y_{C_3}-y_{B_3})^2+(z_{C_3}-z_{B_3})^2=l_4^2 \quad (14)$$

From Eq. (14), we can evaluate θ_3 as following

$$\theta_3 = 2 \arctan\left(\frac{2l_3z_3 \pm \sqrt{4z_3^2l_3^2 - g_3 h_3}}{g_3}\right) \quad (15)$$

Where

$$z_3 = z_{C_3}, \quad g_3 = (l_1-l_3)^2 - l_4^2 + y_{C_3}^2 + z_{C_3}^2,$$

$$h_3 = (l_1+l_3)^2 - l_4^2 + y_{C_3}^2 + z_{C_3}^2$$

We can conclude that this robot has 16 solutions to the inverse kinematic model, twice as many as the Delta robot. This is due to the mobile platform which is made with two parts. For the same position of P , there are two values for β and for each β value, there are two values for θ_1 and θ_2 . However, there are only two θ_3 values in total. The number of solutions in the inverse kinematic model is the product of 4 by 4 by 2, i.e. 16 solutions.

SINGULARITY ANALYSIS

The singularity analysis of parallel robots has been well-documented in the literature. We can find the parallel and serial Jacobian matrix, named A and B respectively [19, 20], by differentiating the constraint equations with respect to time.

Then we obtain the parallel and serial singularities by studying $\det(A)$ and $\det(B)$, respectively [21].

For the mechanism studied, the singularities are similar to those of a Delta robot. A new singular configuration exists because the mobile platform is made in two parts. When β is equal to $\pi/2$ or $3\pi/2$, the robot admit a new singular configuration because the determinant of the parallel Jacobian matrix A vanished. This defines in the workspace, a vertical plane passing through the origin and parallel to the plane (xz).

CASE STUDY

To illustrate this study, we refer to the dimension parameters of the ABB robot 14R, i.e., $l_1=300$, $l_2=70$, $l_3=350$, $l_4=800$, $l_5=100$, $l_6=10$ and $l_7=50$. Its parallel and serial singularity can be computed with the Siropa library [22]. The determinant of matrix A can be written

$$\sin(\beta)(35\cos(\theta_3)-x_{c_1}+16)x_{c_1}(35\sin(\theta_2)-z_{c_1})=0 \quad (16)$$

and that of matrix B as

$$\begin{aligned} &(-2100S_{\theta_1}-70z_{c_1}C_{\theta_1})(1400S_{\theta_2}-70z_{c_1}C_{\theta_2}) \\ &(350C_{\beta}S_{\theta_3}+70x_{c_1}S_{\theta_3}-1120S_{\theta_3}-70z_{c_1}C_{\theta_3})C_{\beta}=0 \end{aligned} \quad (17)$$

By using Groebner base elimination methods, these surfaces can be plotted in the Cartesian space. Figure 4 depicts the singular configurations in the Cartesian space and Fig. 5 the serial singularities with a different color for each term of the Eqs (15) and (16).

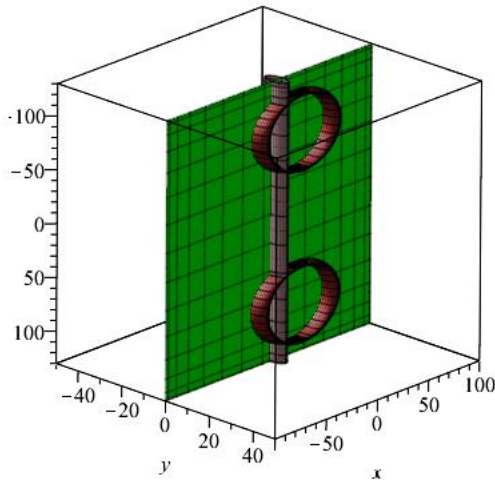


FIGURE 4. PARALLEL SINGULARITIES OF THE ROBOT

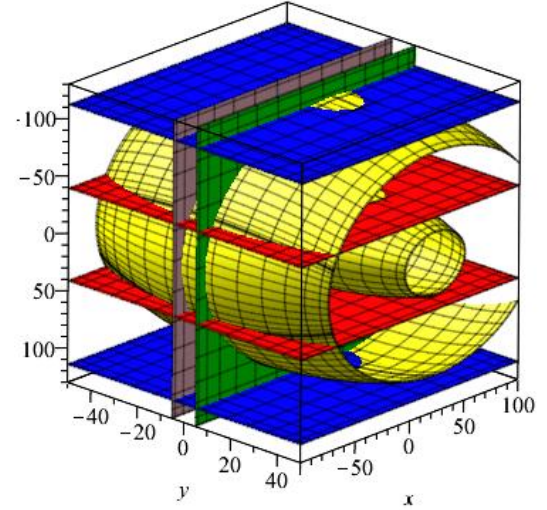


FIGURE 5. SERIAL SINGULARITIES OF THE ROBOT

CONCLUSIONS

In this article, a new asymmetrical new parallel mechanism of pure parallel translation with a degree of zero coupling and complete motion decoupling has been proposed. The inverse and direct kinematic models are obtained. The mechanism is simple in structure and easy to manufacture, which can be used in transportation, positioning and other operations of the manufacturing industry. The study of singular configurations is simple because of the independence of the kinematic chains.

ACKNOWLEDGMENTS:

This research is sponsored by the NSFC (Grant No. 51475050 and No. 51375062) and Jiangsu Key Development Project (No.BE2015043).

REFERENCES

- [1] Liu X., Wang J., Kinematic and workspace analysis of a new type of spatial 3-DOF parallel mechanism. *Journal of Mechanical Engineering*, 2001, 37(10):36-39.
- [2] Clavel R., A Fast Robot with Parallel Geometry // *Proc. Int. Symposium on Industrial Robots*. 1988:91-100.
- [3] Stock M, Miller K, Optimal Kinematic Design of Spatial Parallel Manipulators: Application to Linear Delta Robot. *Journal of Mechanical Design*, 2003, 125(2):292-301.
- [4] Bouri M, Clavel R., The Linear Delta: Developments and Applications // *Robotics*. VDE, 2010:1-8.

- [5] Kelaiaia R, Company O, Zaatri A., Multiobjective optimization of a linear Delta parallel robot. *Mechanism & Machine Theory*, 2012, 50(2):159–178.
- [6] Tsai L. W, Walsh G C., Stamper R E., Kinematics of a Novel Three DOF Translational Platform. 1996, 4:3446-3451.
- [7] Chablat D. and Wenger P., Architecture Optimization of a 3-DOF Parallel Mechanism for Machining Applications, the Orthoglide, *IEEE Transactions On Robotics and Automation*, 19(3):403-410, June, 2003.
- [8] Caro S., Chablat D., Lemoine P., Wenger P., Kinematic Analysis and Trajectory Planning of the Orthoglide 5-Axis, *Proceedings of the ASME 2015, International Design Engineering Technical Conferences & Computers and Information in Engineering Conference*, Aug 2015, 2015.
- [9] Li S, Huang Z, Zuo R., Kinematics of a Special 3-DOF 3-UPU Parallel Manipulator // *ASME 2002 International Design Engineering Technical Conferences and Computers and Information in Engineering Conference*. 2002:1035-1040.
- [10] Zhao T., Huang Z., Kinematics analysis of a three dimensional mobile parallel platform mechanism. *China Mechanical Engineering*, 2001, 12(6):612-616.
- [11] Zhao Y., Dimensional synthesis of a three translational degrees of freedom parallel robot while considering kinematic anisotropic property. *Robotics and Computer-Integrated Manufacturing*, 2013, 29(1):169-179.
- [12] Zeng Q, Ehmann K F, Cao J., Tri-pyramid Robot: Design and kinematic analysis of a 3-DOF translational parallel manipulator. Pergamon Press, Inc. 2014.
- [13] Qiang Z., Ehmann K F., Jian C., Tri-pyramid Robot: stiffness modeling of a 3-DOF translational parallel manipulator. *Robotica*, 2016, 34(2):383-402.
- [14] Lee S, Zeng Q, Ehmann K F., Error modeling for sensitivity analysis and calibration of the tri-pyramid parallel robot. *International Journal of Advanced Manufacturing Technology*, 2017(5):1-14.
- [15] Bhutani G, Dwarakanath T A., Novel design solution to high precision 3 axes translational parallel mechanism. *Mechanism & Machine Theory*, 2014, 75(5):118-130.
- [16] Li W., Gao F., Zhang J., A three-DOF translational manipulator with decoupled geometry. Cambridge University Press, 2005.
- [17] Shen H., Xiong K., Kinematic decoupling design method and application of parallel mechanism. *Trans. of The Chinese Society of Agricultural Machinery*, 2016, 47(6):348-356.
- [18] Yang T., Liu A., Shen H., et.al, Topology design of robot mechanism. Springer, 2018.
- [19] Gosselin C., and Angeles J., Singularity analysis of closed-loop kinematic chains, in *IEEE Transactions on Robotics and Automation*, 6(3), pp. 281–290, June 1990.
- [20] Wenger Ph., Chablat D., Definition sets for the direct kinematics of parallel manipulators, *8th International Conference in Advanced Robotics*, pp. 859-864, 1997.
- [21] Chablat D., Wenger Ph., Working modes and aspects in fully-parallel manipulator, *Proceedings of IEEE International Conference on Robotics and Automation*, pp. 1964–1969, May 1998.
- [22] Siropa, Algebraic and robotic functions, <http://siropa.gforge.inria.fr/doc/files/siropa-mpl.html>, 2018.